

Effect of textural and chemical characteristics of activated carbons on phenol adsorption in aqueous solutions

Diana P. Vargas¹, Liliana Giraldo², Juan Carlos Moreno-Piraján^{3*}

¹University of Tolima, Grupo de Materiales Porosos Para Aplicaciones Ambientales y Tecnológicas, Chemistry Department, Faculty of Science, Ibagué, Colombia

²National University of Colombia, Grupo de Calorimetría, Chemistry Department, Faculty of Science, Bogotá, Colombia

³Andes University, Grupo de Sólidos Porosos y Calorimetría, Chemistry Department, Faculty of Science, Bogotá, Colombia

*Corresponding author: e-mail: jumoreno@uniandes.edu.co

The effect of textural and chemical properties such as: surface area, pore volume and chemical groups content of the granular activated carbon and monoliths on phenol adsorption in aqueous solutions was studied. Granular activated carbon and monolith samples were produced by chemical activation. They were characterized by using N₂ adsorption at 77 K, CO₂ adsorption at 273 K, Boehm Titrations and immersion calorimetry in phenol solutions. Microporous materials with different pore size distribution, surface area between 516 and 1685 m² g⁻¹ and pore volumes between 0.24 and 0.58 cm³ g⁻¹ were obtained. Phenol adsorption capacity of the activated carbon materials increased with increasing BET surface area and pore volume, and is favored by their surface functional groups that act as electron donors. Phenol adsorption capacities are in ranged between 73.5 and 389.4 mg · g⁻¹.

Keywords: activated carbon monoliths, phenol adsorption, textural and chemical characteristics, immersion calorimetry.

INTRODUCTION

Water pollution is a major environmental problem. Human activities have generated high amount of substances that can accumulate in the water, altering its natural balance and affecting its biodiversity. Those pollutants include heavy metals, dyes, pesticides, plastics, and other organic substances. Phenols are organic compounds highly toxic and difficult to biodegrade, even at low concentration, presenting a high risk to the health of all living beings¹. Phenol and phenolic compounds are raw materials or intermediates in numerous petrochemical, chemical and pharmaceutical industries, and are likewise oxidative degradation products of aromatic hydrocarbons with high molecular weight. Therefore, they are one of the most important pollutants in wastewater coming from the industrial activity and strong limits are set for their acceptable levels in wastewaters^{2,3}. Contact with phenols can cause respiratory irritation, headaches, burning eyes, skin burns, liver damage, dark urine, irregular heartbeat, and also a negative effect on the central nervous system, causing dead in some cases. Hence, it is essential to remove phenols from wastewaters before being released to the environment.

Effective treatment of industrial wastewater has gained much interest in recent decades due to the growing awareness of environmental protection and also because environmental regulations have been strengthened. Therefore, it is necessary to develop effective technologies to eliminate pollutants and intensify the research and development field. There are different technologies for the treatment of phenol contaminated waters including biodegradation¹, oxidative degradation⁴, membrane filtration⁵, photocatalytic degradation⁶, photo-Fenton⁷, and adsorption^{2,3,8}. Wet oxidation and catalytic wet oxidation (using air and pure oxygen) have been widely used along with the Fenton process for phenol elimination. Although the Fenton process has high values of phenols removal, it comes with some drawbacks such as the excessive use of hydrogen peroxide and the need to remove the

added iron, involving an additional step in the process, increasing the cost.

Adsorption is considered as an alternative for water phenol removal⁹. Many types of adsorbents have been developed for this purpose: clays such as montmorillonite and bentonite¹⁰, zeolites¹¹, metal organic frameworks (MOFs)¹², mesoporous silica¹³, nanoparticles¹⁴, and activated carbons^{15, 16}. Activated carbons are of great interest, because of its versatility and properties. It has a large surface area, high porosity development of different sizes and a heterogeneous surface chemistry. An advantage of the carbonaceous materials over other solids is the ease in adjusting its textural and chemical characteristics during the preparation process.

The aim of this work was to study the effect that have the textural and chemical properties (BET surface area, pore volume and chemical groups content) of granular activated carbon and monoliths on the phenol adsorption in aqueous solution. Granular and monolith activated carbon samples were produced by chemical activation of African Palm Stone with H₃PO₄ and ZnCl₂ solutions at different concentrations. The characterization of these materials was done by using N₂ adsorption at 77 K, CO₂ adsorption at 273 K, Boehm Titrations and immersion calorimetry in phenol solutions. The phenol adsorption capacity was related with the textural and chemical parameters determined by the characterization techniques.

EXPERIMENTAL SECTION

Synthesis of activated carbons

The African palm stone was used as the lignocellulosic precursor. It was washed and crushed to a particle size of 2–3 mm for granular activated carbon and to 38 μm for activated carbon monoliths. It was impregnated with the activating agents (H₃PO₄ 32% w/v and ZnCl₂ 48% w/v) at 358 K during 6 hours¹⁷. Then, it was carbonized in a N₂ atmosphere at 723 K (those impregnated with H₃PO₄) and 773 K (those impregnated with ZnCl₂), and

finally washed. The activated carbon monoliths were prepared using a process of compaction, the precursor impregnated is leads to a uniaxial press and is subjected to a pressure of 4500 psi and a temperature of 423 K, hot pressing to take advantage of the tar binders generated during the precursor impregnation and thus avoid the use of an additional substance.

Eight samples of activated carbon were obtained. They were identified as GC for granular carbon, M for monoliths, P or Zn for H_3PO_4 and ZnCl_2 activating agent respectively and a number that indicates the concentration of the substance. Figure 1 shows the obtained carbonaceous materials.



Figure 1. Carbonaceous materials a) granular activated carbon, b) activated carbon monoliths

Characterization

Table 1 shows the techniques used to obtained textural and chemical characteristics of activated carbons prepared^{18, 19}.

Table 1. Characterization techniques

N ₂ adsorption at 77 K	•Quantachrome, Autosorb 3-B, Outgassing of samples at 523 K for 24h
CO ₂ adsorption at 273 K	•Quantachrome, Autosorb 3-B, Outgassing of samples at 523 K for 24h
Boehm titrations	•100 mg adsorbent, 25 mL solutions NaOH, NaHCO ₃ , Na ₂ CO ₃ and HCl 0.1 M, T= 298 K, t= 40 hours. Constant stirred
Point of Zero Charge	•Mass titration method (Noh y Schwarz). 0.05-0.3 g of sample NaCl 0.1 N (10 mL), T= 298 K, t= 48 hours
Immersion calorimetry	•0.1 g adsorbent., C ₆ H ₆ , (8 mL), T= 298 K
Phosphorus and Zinc Quantification	•Phosphorus: Spectrophotometric method Zinc: Atomic Absorption

Phenol Adsorption

The phenol adsorption capacity of the obtained carbonaceous materials was determined using discontinuous systems. 500 mg of activated carbon and 250 mL of phenol aqueous solution at a concentration of 500 and 1000 mg L⁻¹ were placed in each glass bottle. The samples were mechanically stirred and maintained at a temperature of 25°C for a period of about 72 hours. The equilibrium concentration of phenol in the solutions after adsorption, was determined in a UV-Vis spectrophotometric equipment at a wavelength of 271 nm (Spectronic Genesys Milton Roy Co. SN).

Immersion enthalpy determination

The immersion enthalpy of the activated carbons were determined by using phenol solutions of 500 mgL⁻¹ and 1000 mgL⁻¹. For this purpose 100 mg of sample were used and added to 8 mL of phenol solution, for the

calorimetric determination was used a heat conduction microcalorimeter with a stainless steel calorimetric cell²⁰.

RESULTS AND DISCUSSION

Textural and Chemical characteristics

Figure 2 shows the N₂ adsorption isotherms of the prepared activated carbons at 77K. GCP48, GCP32, MP48 and GCZn32 samples have isotherms type Ib, this type of isotherm is characteristic of materials with pore size distributions over a broader range including wider micropores and possibly narrow mesopores. Meanwhile MP32, MZn32, GCZn48 and MZn48 samples have type Ia isotherms, materials that have mainly narrow micropores according with the last IUPAC classification¹⁸.

There is an influence of the activating agent in the textural characteristics of the carbonaceous materials. According to the results, the H_3PO_4 activation generates a wide porosity development, while the ZnCl_2 gave rise to activated carbons with narrow porosity. The obtained surface areas are between 516 and 1685 m² g⁻¹ and pore volumes between 0.24 and 0.58 cm³ g⁻¹.

Table 2 shows the textural characteristics of the carbonaceous materials. It is evident that the monoliths have lower S_{BET} , V_0 , V_{meso} , $V_{0.99}$ and V_n compared to granular materials prepared under the same conditions. Such behavior can be attributed to the pressing process to

which the impregnated material was subjected to form the monoliths. Others authors have shown¹⁷ that the effect of forming pressure on the development of porosity in the monoliths, is mainly due to changes that the impregnation produces on the physicochemical properties of the precursor. The activating agents separate the cellulose fibers and causes partial hemicellulose and lignin (the main components of the precursor) depolymerization, which leads to a decrease in mechanical strength. Both factors lead to swelling of the particle. Once the material is impregnated, the carbon conversion starts and a significant amount of tar on the particles surface is observed. Tars come from the depolymerization of the cellulose, followed by dehydration and condensation. Process that is catalyzed by the impregnating agents and lead to the crosslinking and expansion of the structure. When the solution is evaporated, the particle precursor has relatively weak structure. At that moment, all the

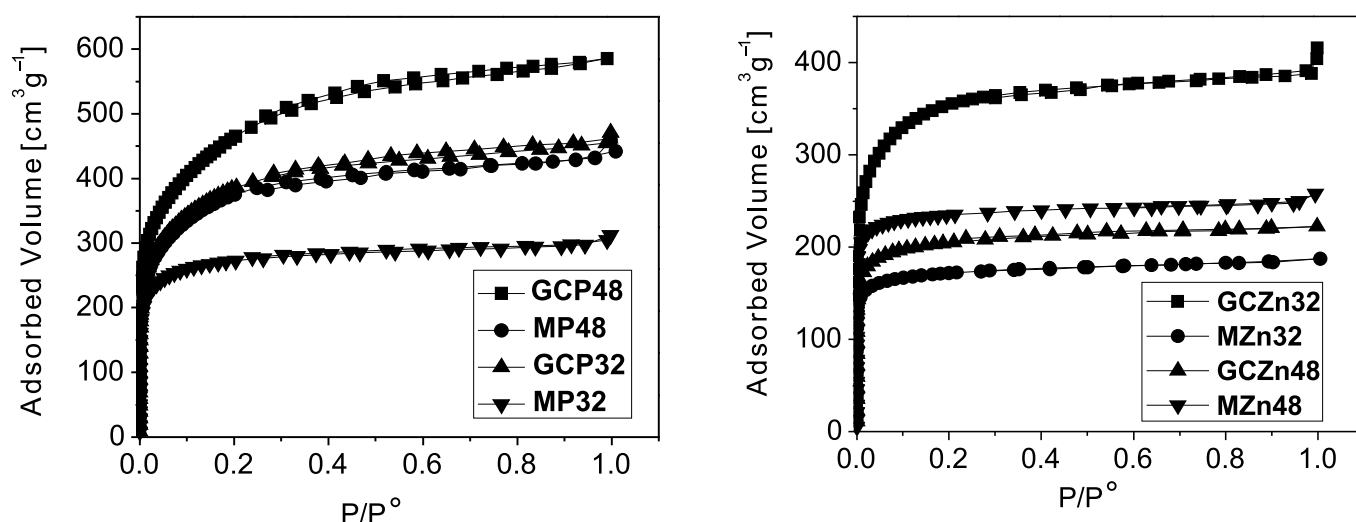


Figure 2. Nitrogen adsorption isotherms at 77 K for the obtained activated carbons

Table 2. Textural parameters for the carbonaceous materials obtained from the N_2 adsorption isotherm at 77 K and CO_2 adsorption isotherm at 273 K

N ₂ Adsorption at 77 K					CO ₂ Adsorption at 273 K
Sample	$S_{BET} / [m^2 g^{-1}]$	$V_O / [cm^3 g^{-1}]$	$V_{meso} / [cm^3 g^{-1}]$	$V_{0.99} / [cm^3 g^{-1}]$	$V_n / [cm^3 g^{-1}]$
GCP32	1407	0.50	0.23	0.73	0.34
GCP48	1685	0.58	0.33	0.91	0.42
MP32	1020	0.40	0.09	0.49	0.25
MP48	1368	0.48	0.18	0.66	0.32
GCZn32	1314	0.50	0.05	0.55	0.30
GCZn48	516	0.24	0.02	0.26	0.23
MZn32	660	0.26	0.03	0.29	0.23
MZn48	924	0.37	0.01	0.38	0.36

chemical agent is inside the structure and surrounded by tars. By applying pressure to the impregnated precursor at a temperature of 423 K, additional loss of water and tars from the interior of the particle is produced, leading to a decrease of space in the structure and therefore the development of mesoporosity that is observed in the granular series (Figs. 4–5a). All of this is the result of the pressure employed during the monoliths production.

Pore size distribution

Figure 3 shows the pore size distributions of the carbonaceous materials obtained from the experimental data of nitrogen adsorption at 77 K. Microscopic models (Functional Theory of Non-Local Density (NLDFT) and Functional Theory of Solid Reacted Density (QSDFT)) were used to describe the adsorption and fluids behavior of the pores at Molecular level²¹. Good fit of the data were found in all samples when using the QSDFT model. This model yielded a percentage of error between 0.21–0.82% different from that calculated by the NLDFT model which corresponds to 1.19–2.61%. The QSDFT

model presents advantages for the determination of the pore size distributions (PSDs) in carbonaceous materials that are chemically and geometrically disordered since it takes into account the effects of surface roughness and heterogeneity²¹.

It was observed that the granular activated carbons prepared with H_3PO_4 had microporosity with pore volumes of less than 2 nm and moderate volumes of mesopores between 2.5–5.0 nm, while the monoliths obtained with the same activating agent had a pore size distribution that consisted mainly of micropores. This could be an evidence that the pressing process decreases the interparticulate space and reduces the mesopores volumes. Those granular activated carbons and monoliths prepared with $ZnCl_2$ showed narrow pore size distributions (<1.5 nm) with no mesopores volumes.

Chemical Characteristics

Table 3 shows the surface functional groups of the activated carbons and the point of zero charge (determined by Boehm titrations). Experimental data indicates the

Table 3. Surface functional groups content and point of zero charge

Sample	Carboxylic acids / $[\mu mol g^{-1}]$	Lactone / $[\mu mol g^{-1}]$	Phenol / $[\mu mol g^{-1}]$	Total Acidity / $[\mu mol g^{-1}]$	Total Basicity / $[\mu mol g^{-1}]$	pH _{PZC}	%P or % Zn
GCP32	143.2	95.99	217.9	457.0	54.72	5.63	0.31
GCP48	153.8	84.01	246.5	484.3	137.5	4.13	4.24
MP32	141.4	55.92	212.0	409.3	29.10	5.32	0.44
MP48	155.5	26.67	256.4	438.5	126.0	3.73	4.70
GCZn32	159.1	0	263.6	422.7	66.73	5.91	0.12
GCZn48	198.6	12.91	172.1	383.6	95.61	5.31	1.25
MZn32	162.2	0	172.3	334.5	31.10	5.88	0.27
MZn48	187.5	18.36	179.8	385.6	92.84	5.24	1.46

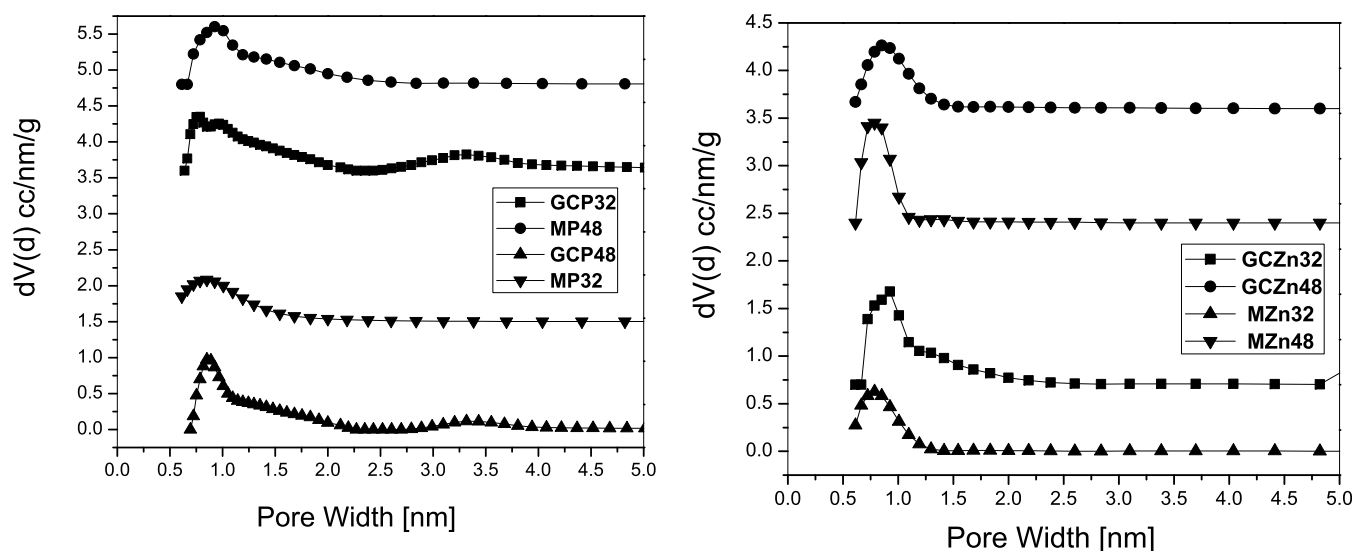


Figure 3. Comparison between the pore size distributions (PSDs) of the prepared samples

changes in the surface chemical properties with respect to the activating agent.

In series prepared with H_3PO_4 , is observed that the increase in concentration of this activating agent, produces an increase in carboxylic and phenolic groups. The number of carboxylic and phenolic groups increased up to 27% at the highest concentration but the content of lactone groups decreased to 52%. The percentage of phosphorous in those samples was between 0.31 and 4.70%. The amount of residual phosphorus increased along with the concentration of the activating agent due to the formation of polyphosphates, phosphates, that generates a strong carbon matrix difficult to remove through the washing process. Those series prepared with $ZnCl_2$ showed an increase carboxylic groups content (up to 19%) and a slightly change in concentration of lactone groups (48%) when increasing of zinc chloride concentration. In samples such as GCZn32 and MZn32 the lactone groups were not detectable by this technique. The residual Zn was between 0.12 and 1.46% and its concentration increases along with the the activating agent concentration due to conformation of a carbonaceous structure.

Immersion Calorimetry

It is a thermodynamic technique that provides information about the interactions between solids and different immersion liquids²². During the process, there is a formation of an adsorbed liquid layer of molecules on the solid surface and the wetting of the adsorbed layer. The intensity of the thermal effect leads to comparisons between different characteristics of porous solids that

can be useful for specific applications. The values of the immersion enthalpies are between -58.37 Jg^{-1} and -181.1 Jg^{-1} .

Table 4 shows that the immersion enthalpy in benzene increases along with the surface area and pore volume, due to of the large surface available to interact with the solvent, which demonstrates that the interaction energy measured by immersion calorimetry is proportional to the BET area determined by nitrogen adsorption.

Based on the immersion enthalpy data of the samples, the accessible surface area was calculated using black coal with a surface area of $30 \text{ m}^2\text{g}^{-1}$. The results were closed to the values calculated for accessible area and BET area obtained by nitrogen sorption measurements. There is also a better correspondence between the surface areas in the samples with structures mainly composed of micropores, that is, those carbonaceous materials prepared using $ZnCl_2$ as impregnating agent. Likewise, a maximum difference of 1% between the surface areas were found. This behavior was adjusted according to the indicated by other authors^{23, 24}. Meanwhile in samples prepared using H_3PO_4 , the difference between surface areas reached values up to 9%, probably because of the higher proportion of mesopores in these carbonaceous materials, which deviates the considerations of the model that were used to calculate the accessible area²⁴.

Phenol adsorption

Figure 4 shows the relation between phenol adsorption capacity of activated carbons and BET area. It is observed that the phenol adsorption capacity of the activated carbons increased with increasing BET surface area. This

Table 4. Immersion enthalpies of the activated carbons in C_6H_6

Sample	Carboxylic acids / [$\mu\text{mol g}^{-1}$]	Lactone / [$\mu\text{mol g}^{-1}$]	Phenol / [$\mu\text{mol g}^{-1}$]	Total Acidity / [$\mu\text{mol g}^{-1}$]	Total Basicity / [$\mu\text{mol g}^{-1}$]	pH _{PZC}	%P or % Zn
GCP32	143.2	95.99	217.9	457.0	54.72	5.63	0.31
GCP48	153.8	84.01	246.5	484.3	137.5	4.13	4.24
MP32	141.4	55.92	212.0	409.3	29.10	5.32	0.44
MP48	155.5	26.67	256.4	438.5	126.0	3.73	4.70
GCZn32	159.1	0	263.6	422.7	66.73	5.91	0.12
GCZn48	198.6	12.91	172.1	383.6	95.61	5.31	1.25
MZn32	162.2	0	172.3	334.5	31.10	5.88	0.27
MZn48	187.5	18.36	179.8	385.6	92.84	5.24	1.46

could be associated with the relation between the surface area and microporosity. The greater the surface are, the greater the microporosity, favoring phenol adsorption²⁵.

Additionally, the relationship between the narrow microporosity volume and the phenol adsorption can be explained by using the pore size distributions of the carbonaceous materials. In this sense, it is observed that the activated carbon of the GCZn and MZn series have pore size volumes below 1.25 nm and have the lowest phenol adsorption capacities compared to those obtained for the GCP series and MP, which have a greater pore size distribution, this fact can be explained due to the size of the molecule of phenol 0.75 nm, that is, in activated carbon samples prepared with ZnCl_2 there are kinetic restrictions due to the size of the adsorbate, whereas by using H_3PO_4 phenol penetration to the carbonaceous matrix is facilitated by the presence of pores larger than 1.5 nm. An amount of the adsorbed phenol between 73.5 and 389.4 $\text{mg} \cdot \text{g}^{-1}$ was obtained.

It is well known that the sorption process on carbonaceous materials not only depends on their textural characteristics, but also on their surface chemistry and the specific interactions adsorbate-adsorbent. In this

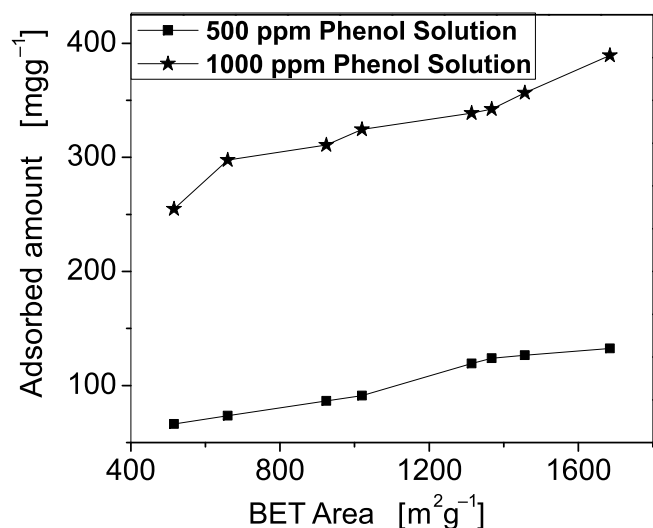


Figure 4. Relation between the amount of phenol adsorbed and BET area of the samples

study some chemical activated carbons characteristics were correlated with the phenol adsorption capacity.

Figure 5 shows the amount of the adsorbed phenol. This feature is affected by the presence of surface groups as evidenced by this work. Total acidity decreases as the content of carboxyl and phenolic groups (electron acceptors) decreases, observing an increase the adsorbed amount of phenol due to the availability of the π electrons on the graphene layers that interact only with the phenol molecule, and thus favors its interaction with the carbonaceous materials, increasing the adsorbed amount. Phenol adsorption capacity is favored by the surface functional groups of the activated carbon that act as electron donors and offers its electrons to the phenol aromatic rings (electron acceptors); enabling the establishment of the donor-acceptor complex for the primary bonding mechanism between the pollutant and the adsorbent²⁶.

Figure 6 shows the thermograms obtained for the activated carbons with the highest and lowest immersion enthalpy values in phenol solutions. The differences in the size of the immersion peaks are related with the

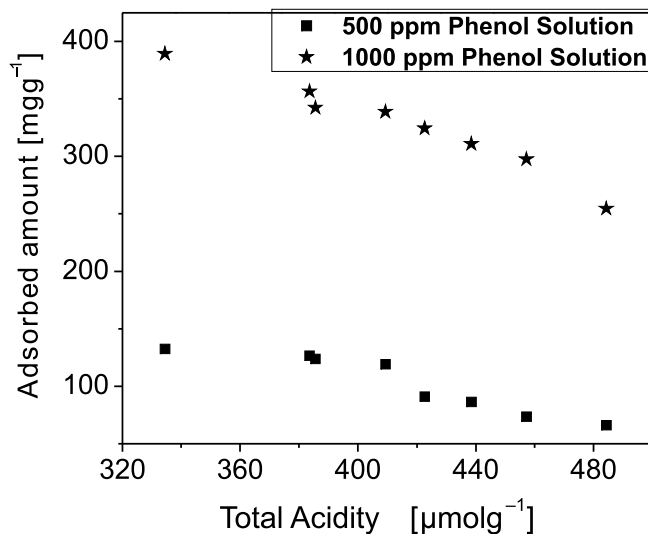


Figure 5. Relation between the adsorbed amount of phenol and Total Acidity

adsorbate-adsorbent interaction and the adsorption capacity of the solids.

Figure 7 shows the relation between the immersion enthalpies from 500 ppm phenol and 1000 ppm solutions and the amount of adsorbed phenol. There is an increase in the immersion enthalpy along with the phenol adsorp-

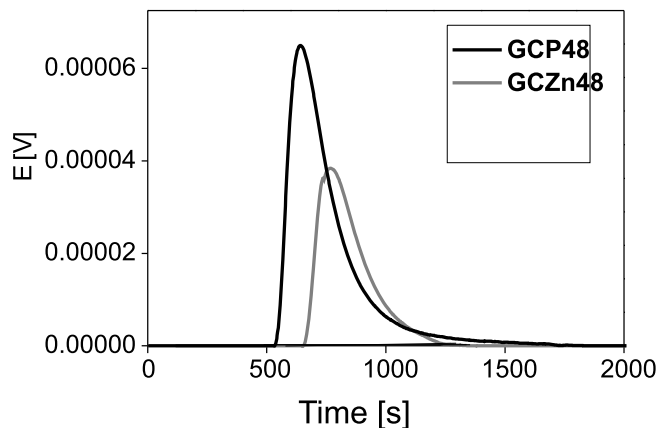


Figure 6. Comparison between the immersion enthalpy thermograms from 1000 ppm phenol solution

tion capacity in the activated carbons. This behavior is consistent with the exothermic nature of the adsorption process when the carbonaceous material interacts with phenol molecule. The immersion enthalpies are among -38.76 and -123.42 Jg^{-1} .

CONCLUSIONS

The influence of the textural and chemical characteristics of the different activated carbons on the phenol

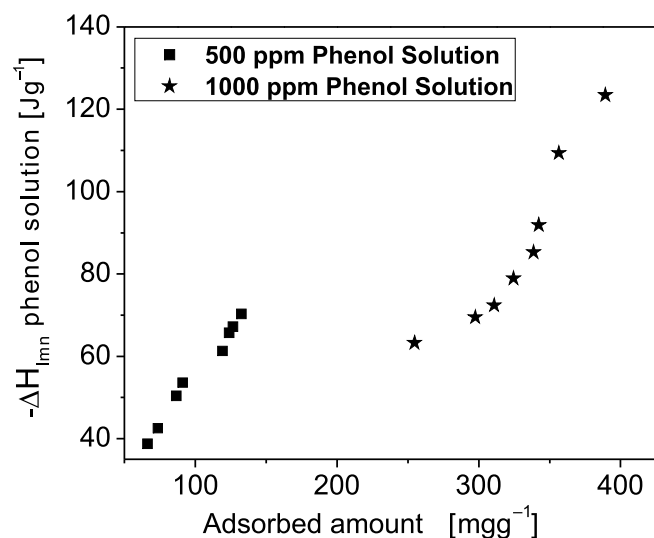


Figure 7. Relation between the immersion enthalpies of phenol solutions and the amount of adsorbed molecule

adsorption capacity was studied. Activated carbons had surface areas between 516–1685 m²g⁻¹ and pore volumes between 0.24 to 0.58 cm³g⁻¹. The results showed that the activating agents (ZnCl₂ and H₃PO₄) made the carbonaceous materials to have different characteristics. ZnCl₂ gave rise to narrow microporosity, while H₃PO₄ developed wide porosity.

It is established that phenol adsorption capacity is associated to the presence of pores with a size larger than 1.5 nm, since it favors its access to phenol molecules with diameters of 0.75 nm. Another important element is the surface chemistry of materials including total acidity, which affects the interaction between the surface area of the activated carbon and the phenol molecules. The monolith activated carbons obtained by using H₃PO₄ (48%) were the best materials for Phenol adsorption, with an adsorption capacity of 389.4 mgg⁻¹. Immersion enthalpies of the activated carbons in benzene can be correlated with parameters determined by gas adsorption. For this reason, immersion calorimetry represents a valuable complement to other carbonaceous materials characterization techniques.

ACKNOWLEDGMENTS

The authors thank the Framework Agreement between the University of Los Andes and the National University of Colombia, as well as the Agreement Statement agreed between the Chemistry departments of these two universities.

LITERATURE CITED

- Basak, B., Bhunia, B. & Dey, A. (2014). Studies on the potential use of sugarcane bagasse as carrier matrix for immobilization of *Candida tropicalis* PHB5 for phenol biodegradation. *Int. Biodeterior. Biodegrad.* 93, 107–117. DOI: 10.1016/j.ibiod.2014.05.012.
- Gupta, A. & Balomajumder, C. (2015). Simultaneous removal of Cr(VI) and phenol from binary solution using *Bacillus* sp. immobilized onto tea waste biomass. *J. Water. Proc. Eng.* 6, 1–10. DOI: 10.1016/j.jwpe.2015.02.004.
- Isaac, W., Mwangi, J., Ngila, C., Ndung'u, P. & Msagati, T.A.M. (2014). Removal of phenolics from aqueous media

using quaternised maize Tassels. *J. Environ. Manag.* 134, 70–79. DOI: 10.1016/j.jenvman.2013.12.031

- Osegueda, O., Dafinov, A., Llorca, J., Medina, F. & Sui-eiras, J. (2015). Heterogeneous catalytic oxidation of phenol by in situ generated hydrogen peroxide applying novel catalytic membrane reactors. *Chem. Eng. J.* 262, 344–355. DOI: 10.1016/j.cej.2014.09.064

- Zagklis, D.P., Vavouraki, A.I., Kornaros, M.E. & Paraskeva, C.A. (2015). Purification of olive mill wastewater phenols through membrane filtration and resin adsorption/desorption. *J. Hazard Mater.* 285, 69–76. DOI: 10.1016/j.jhazmat.2014.11.038.

- Turkia, A., Guillardb, C., Dappozzeb, F., Ksibia, F., Berhaultb, G. & Kochkara, H. (2015). Phenol photocatalytic degradation over anisotropic TiO₂ nanomaterials: Kinetic study, adsorption isotherms and formal mechanisms. *Appl. Catal. B.* 163, 404–414. DOI: 10.1016/j.apcatb.2014.08.010.

- Yu, L., Chen, J., Liang, Z., Xu, W., Chen, L. & Ye, D. (2016). Degradation of phenol using Fe₃O₄-GO nanocomposite as a heterogeneous photo-Fenton catalyst. *Sep. Purif. Technol.* 171, 80–87. DOI: 10.1016/j.seppur.2016.07.020.

- Kamel, S., Abou-Yousef, H., Yousef, M. & El-Sakhawy, M. (2012). Potential use of bagasse and modified bagasse for removing of iron and phenol from water. *Carbohydr. Polym.* 88(1), 250–256. DOI: 10.1016/j.carbpol.2011.11.090.

- Álvarez-Torrellas, S., Martín-Martínez, M., Gomes, H.T., Ovejero, G. & García, J. (2017). Enhancement of p-nitrophenol adsorption capacity through N₂-thermal-based treatment of activated carbons. *Appl. Surf. Sci.* 414, 424–434. DOI: 10.1016/j.apsusc.2017.04.054.

- Ma, L., Zhu, J., Xi, Y., Zhu, R., He, H., Liang, X. & Ayoko, G.A. (2016). Adsorption of phenol, phosphate and Cd(II) by inorganic–organic montmorillonites: A comparative study of single and multiple solute. *Colloid Surf. A.* 497, 63–71. DOI: 10.1016/j.colsurfa.2016.02.032.

- Cheng, W.P., Gao, W., Cui, X., Ma, J.H. & Li, R.F. (2016). Phenol adsorption equilibrium and kinetics on zeolite X/activated carbon composite. *J. Taiwan Inst. Chem. E.* 62, 192–198. DOI: 10.1016/j.jtice.2016.02.004.

- Hasan, Z. & Jhung S.H. (2015). Removal of hazardous organics from water using metal-organic frameworks (MOFs): Plausible mechanisms for selective adsorptions. *J. Hazard. Mat.* 283, 329–339. DOI: 10.1016/j.jhazmat.2014.09.046.

- Mangrulkar, P.A., Kamble, S.P., Meshram, J. & Rayalu, S.S. (2008). Adsorption of phenol and o-chlorophenol by mesoporous MCM-41. *J. Hazard. Mater.* 160(2–3), 414–421. DOI: 10.1016/j.jhazmat.2008.03.013

- Al-Hamdi, A.M., Sillanpää, M., Bora, T. & Dutta J. (2016). Efficient photocatalytic degradation of phenol in aqueous solution by SnO₂: Sb nanoparticles. *Appl. Surf. Sci.* 370, 229–236. DOI: 10.1016/j.apsusc.2016.02.123.

- Thue, P.S., Adebayo, M.A., Lima, E.C., Sieliechi, J.M., Machado, F.M., Dotto, G.L. Vagheti, J.C.P. & Dias, S.L.P. (2016). Preparation, characterization and application of microwave-assisted activated carbons from wood chips for removal of phenol from aqueous solution. *J. Mol. Liq.* 223, 1067–1080. DOI: 10.1016/j.molliq.2016.09.032.

- Zhang, D., Huo, P. & Liu, W. Behavior of phenol adsorption on thermal modified activated carbon. (2016). *Chin. J. Chem. Eng.* 24(4), 446–452. DOI: 10.1016/j.cjche.2015.11.022.

- Nakagawa, Y., Molina-Sabio, M. & Rodríguez-Reinoso, F. (2007). Modification of the porous structure along the preparation of activated carbon monoliths with H₃PO₄ and ZnCl₂. *Micropor. Mesopor. Mater.* 103(1–3), 29–34. DOI: 10.1016/j.micromeso.2007.01.029.

- Thommes, M., Kaneko, K., Neimark, A.V., Olivier, J.P., Rodríguez-Reinoso, F., Rouquerol, J. & Sing, K.W.S. (2015). Physisorption of gases, with special reference to the evaluation of surface area and pore size distribution (IUPAC Technical Report). *Pure Appl. Chem.* 87, 1051–1070. DOI: 10.1515/pac-2014-1117.

19. López, M.V., Stoeckli, F., Moreno-Castilla, C. & Carrasco-Marina, F. (1999). On the characterization of acidic and basic surface sites on carbons by various techniques. *Carbon* 37(8), 1215–1221. DOI: 10.1016/S0008-6223(98)00317-0.
20. Giraldo, L. & Moreno, J.C. (2000) Determination of the Immersion Enthalpy of activated carbon by Microcalorimetry of the Heat Conduction. *Instrum. Sci. Technol.* 28(2), 171–178. DOI: 10.1081/CI-100100970.
21. Neimark, A.V., Lin, Y., Ravikovitch, P.I. & Thommes, M. (2009). Quenched solid density functional theory and pore size analysis of micro-mesoporous carbons. *Carbon* 47(7), 1617–1628. DOI: 10.1016/j.carbon.2009.01.050.
22. Silvestre-Albero, J., Gómez, C., Sepúlveda-Escribano, A. & Rodríguez-Reinoso, F. (2001). Characterization of microporous solids by Immersion calorimetry. *Colloid Surf. A.* 187–188, 151–165. DOI: 10.1016/S0927-7757(01)00620-3.
23. Stoeckli, F. & Centeno, T.A. (1997). On the characterization of microporous carbons by immersion calorimetry alone. *Carbon*, 35(8), 1097–1100. DOI: 10.1016/S0008-6223(97)00067-5.
24. Denoyel, R., Fernandez-Colinas, J., Grillet, Y. & Rouquerol, J. (1993). Assessment of the surface area and microporosity of activated charcoals from immersion calorimetry and nitrogen adsorption data. *Langmuir* 9(2), 515–518. DOI: 10.1021/la00026a025.
25. Navarrete, L., Giraldo, L. & Moreno, J.C. (2006). Influencia de la química superficial en la entalpía de inmersión de carbones activados en soluciones acuosas de fenol y 4-nitro fenol. *Rev Colomb Quím.* 35(2), 215–224. DOI: 10.1007/s10973-006-7524-3.
26. Moreno-Castilla, C (2004). Adsorption of organic molecules from aqueous solutions on carbon materials. *Carbon* 42(1), 83–94. DOI: 10.1016/j.carbon.2003.09.022.